Phonon Focusing and Mode-Conversion Effects in Silicon at Ultrasonic Frequencies

A. G. Every,[1,a] Wolfgang Sachse,[1] K. Y. Kim,[1] and M. O. Thompson[2]
[1]*Department of Theoretical and Applied Mechanics, Cornell University, Ithaca, New York 14853*
[2]*Department of Materials Science and Engineering, Cornell University, Ithaca, New York 14853*
(Received 15 May 1990)

Using a scanned point-source, point-receiver technique based on laser generation and piezoelectric sensing, we have observed pronounced anisotropy in the amplitudes of ultrasonic waves propagated in silicon single crystals. The source of this anisotropy can be attributed to focusing of acoustic-ray vectors brought about by the elastic anisotropy of the medium. We present our results in the form of scan images which contain a wealth of structures corresponding to reflection and mode-conversion processes. Head waves are also clearly identified for the first time in a single-crystal specimen. Our results are well accounted for with Monte Carlo ray simulations.

PACS numbers: 62.30.+d, 62.65.+k, 81.40.Jj

The phase and group velocities of acoustic waves in elastically anisotropic solids are not in general equal, even in the absence of dispersion and attenuation. One of the striking consequences of this fact is the phenomenon of focusing, whereby the energy flux radiated by a localized source of acoustic waves is much more highly concentrated in some directions than in others. In many crystals focusing is capable of rendering a superposition of waves with a smooth distribution of wave normals into a flux pattern containing caustics where the ray density is mathematically infinite. This concept has found its most fruitful application in the area of phonon transport, where it is known as phonon focusing.[1,2] Its consequences are vividly displayed in the many phonon images of crystals that can be found in the literature.[3,4]

Anisotropy focusing may be approached from either a geometrical point of view using ray constructs,[3,4] or treated in the context of dynamic Green's functions evaluated in the far field on the basis of the stationary-phase approximation.[5,6] It is implicit in both approaches that focusing is not confined to any particular frequency domain. The essential requirement is that the source-detector distance greatly exceed the dominant wavelength of the acoustic radiation. This condition is easily met with thermal phonons of wavelength $\lambda \simeq 10^{-8}$ m and sample dimensions $l \simeq 10^{-2}$ m, and we note that even at MHz ultrasonic frequencies it can be satisfied without having to resort to inordinately large samples. For instance, taking a frequency of 5 MHz and a medium of wave speed $v = 5000$ m/s, and setting $l = 10\lambda$ yields a modest path length of 10^{-2} m.

Surprisingly, in view of the very striking effects that anisotropy focusing gives rise to, little attention has been given to this phenomenon in texts on ultrasonics. Some account has been taken of focusing in the calculation of the diffraction patterns of finite aperture sources of bulk and surface waves, but as far as we are aware, there are no published accounts of the type of focusing phenomena we describe here.

In this paper we report on pronounced acoustic-wave focusing that we have observed in silicon single crystals using a scanned broadband ultrasonic point-source, point-receiver technique. Our experimental setup is a variation of a method that has been described in greater detail previously.[7] A Q-switched Nd-doped yttrium aluminum garnet laser ($\lambda = 1.06$ μm) provides pulses of $\simeq$4-ns duration and $\simeq$10-mJ energy with a duty cycle of about 1 s. The laser beam is focused to a diameter of $\simeq$0.5 mm on one face of a disk-shaped single crystal of silicon to generate acoustic waves in the sample. The energy density is intentionally kept below the melt threshold ($\simeq 1$ J/cm^2), and the operating conditions lie within the photoacoustic regime.[8] The laser light is absorbed within a thin layer at the surface, causing a temperature rise and free thermoelastic expansion normal to the surface. Lateral expansion of the surface layer is constrained by the underlying material, giving rise to lateral compressive stresses. The wave fields that are generated by such transient forces in *isotropic* solids for various sample geometries have been studied in great depth and are well understood.[9] Of particular note is that sharp spikes or discontinuities occur at the predicted arrival times of longitudinal and transverse waves and of waves which have been reflected with or without undergoing mode conversion.

In the experiments to be described, the ultrasonic signals are detected with a small ($\simeq$1.3 mm diam) piezoelectric transducer (PZT). The voltage signals obtained from the sensor correspond approximately to the normal component of the velocity of the sensed surface, but they are overlayed with damped oscillations, or "ringing," which is initiated by sharp spikes or discontinuities in the surface velocity. The onset of ringing can be measured to an accuracy of $\simeq 0.03$ μs indicating that it is principally comprised of Fourier components of frequency $\simeq$10 MHz.

Compared with the extensive literature on isotropic solids, there is comparatively little known about the tran-

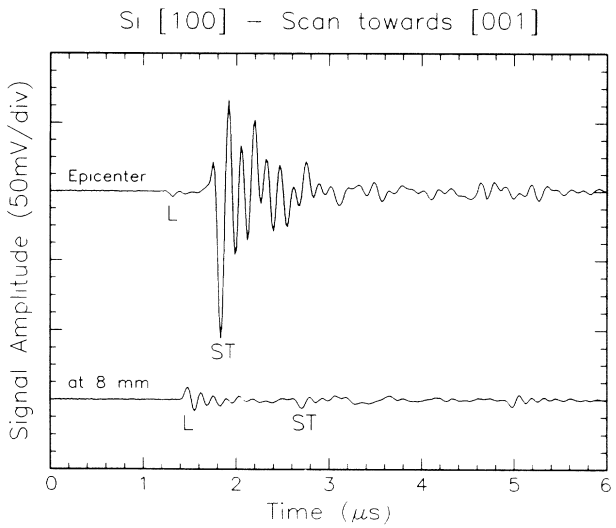

FIG. 1. Wave forms obtained with a [100]-oriented silicon single crystal.

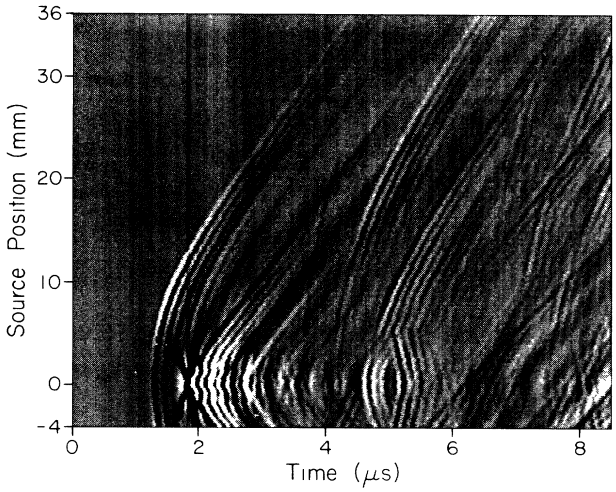

FIG. 2. A scan image obtained with a [100]-oriented silicon single crystal.

sient wave forms and dynamic Green's functions of elastically anisotropic solids. There have been some general treatments of elastic continua and half spaces,[5,6,10,11] but the difficulties posed by the presence of boundaries and the variability permitted by anisotropy seem to have deterred closer attention being given to practical geometries. At present there is no library of theoretical wave forms that we can draw on for comparison with our experimental results. We have therefore restricted our attention to signal onsets which can be associated with wave arrivals, and calculated on the basis of group velocities. Since it is principally the higher-frequency Fourier components that are emphasized at the onsets, it is precisely here that we expect focusing to play its most important role.

Figure 1 shows wave forms detected at epicenter, i.e., directly opposite the point of excitation, and 8 mm off epicenter of a [100]-oriented disk-shaped silicon single crystal of thickness 0.991 cm. The longitudinal- (L) and slow-transverse- (ST) wave arrivals are readily identified. Because of focusing effects, the ST signal is much larger at epicenter than for the other direction. At later times there are other features in the signals which can be identified as various multipass modes. However, because of noise (which can be reduced by signal averaging) and ringing (which cannot), the identification of these later arrivals is more subject to uncertainty.

The interpretation of wave-form data is facilitated by stacking together a large number of wave forms obtained from a closely spaced set of excitation points or viewing directions. Figure 2 shows a scan image generated from 201 wave forms for a set of excitation points located 0.2 mm apart along a line in the [001] direction, and extending from 4 mm on one side of epicenter to 36 mm on the other. A grey scale has been used to represent the signal amplitude. In this image, signal onsets can be easily distinguished from transducer ringing and noise.

The more prominent structures in this image can all be accounted for on the basis of ray arrivals. Our analysis is similar to that used in phonon-imaging calculations.[3,4] A large number of wave normals ($\simeq 10^6$), uniformly distributed in direction, are generated. For each of these normals, starting from Christoffel's equations, one obtains the L, ST, and fast transverse (FT) phase velocities, their polarization vectors, and their group velocities.[12] Based on the group velocities, a distribution function of ray arrival times is determined for each source and receiver configuration. This process corresponds to adding wave intensities without regard to phase relationships between the individual waves and yields an energy flux. For meaningful comparison with our experimental signals, which are a measure of (velocity) amplitude, we take the square root of this distribution function. On this basis we can hope to account for the location and magnitude of the singular features of

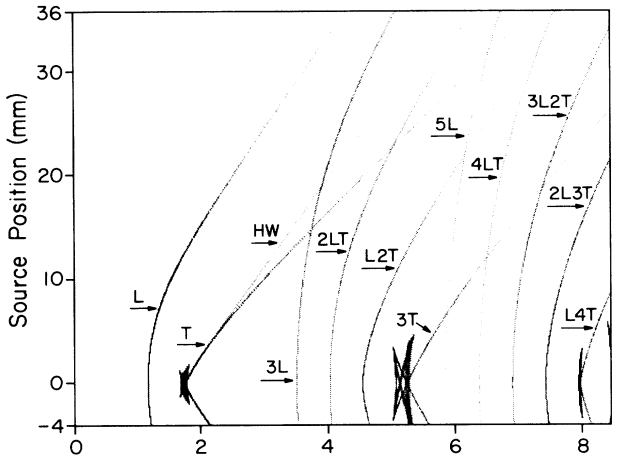

FIG. 3. Calculated scan image corresponding to Fig. 2.

the signal, but not its complete shape.

Figure 3 shows a calculated scan image based on the parameters of the experiment.[13] It contains L and ST single-pass waves, as well as three- and five-pass waves constructed from all possible L and ST segments. The label 2LT, for instance, denotes a wave which has passed 3 times through the crystal, twice as an L wave and once, as a result of mode conversion at the surface, as an ST wave. Figure 3 is in very good agreement with Fig. 2.

Figure 4 shows the scan line in relation to the calculated focusing pattern for [100]-oriented silicon, i.e., the distribution function of the positions of single-pass ray arrivals. Prominent ST and FT focusing structures are labeled. Interestingly, for this particular crystal orientation and scan direction, there is no discernible presence of FT waves in the experimental scan image, in spite of the fact that the scan line lies within a region of intense FT focusing. The reason for this is that the FT waves that would contribute all have polarization vectors lying very nearly perpendicular to the sagittal plane, i.e., the plane containing the wave normal and the normal to the surface.[14] To a good approximation such shear horizontal (SH) waves are not excited by the radial lateral stresses at the source, they cannot participate in mode conversion, and since they do not produce any normal displacement of the surface, they are not detectable by our sensor. We have done calculations in which the source and detector selectivity is accommodated by projecting each mode polarization onto the sagittal plane, and we find that the FT signal is indeed reduced to a negligible amplitude. For other crystal orientations and scan lines there are cases where both FT and ST waves are permitted, and even cases where the ST signal is reduced to a negligible amplitude. These predictions are confirmed by experiment.

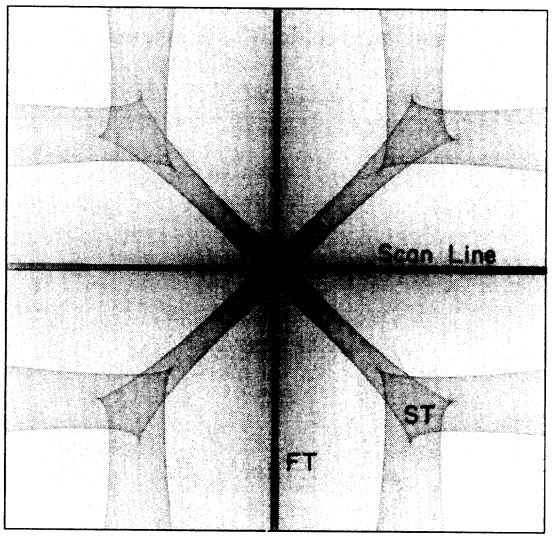

FIG. 4. Focusing pattern of ST and FT waves for a [100]-oriented silicon single crystal.

In comparing Figs. 2 and 3, it is particularly noteworthy that the calculations explain the intense ST structure in the experimental scan image near epicenter. This is a consequence of the intense focusing that occurs near the [100] direction in silicon. In Fig. 4 the focusing of Fig. 3 shows up as the "boxlike" structure at the center, through which the scan line passes. This is a prominent structure in the phonon-focusing patterns of many crystals.[15] At its maximum, the ST signal is $\simeq 30$ times greater than the ST signal in other directions in which there is compensatory defocusing (if one corrects for surface directivity,[8] the focusing enhancement is even larger). This corresponds to an intensity ratio of 3 orders of magnitude, which is comparable to, if not greater than, the intensity magnifications encountered in phonon imaging.

A striking feature in the multipass signals is the 3T structure near epicenter. While all the other multipass structures are convex, this one is concave and, moreover, it terminates abruptly a few mm off epicenter. This structure arises from the complex folded shape of the ST sheet of the wave surface near the [100] direction.

The calculated shapes of all the multipass structures are in good agreement with experiment. An important contributory factor influencing the relative amplitudes of these various structures, at least near epicenter, is that the generation mechanism favors the radiation of ST waves, while the receiver has greater sensitivity for detecting L waves. This, in essence, explains the prominence of mode-conversion structures which provide a means for satisfying both requirements.

At distances greater than about 4 mm ($\simeq 20°$) from epicenter there is an L and ST head wave. This wave may be thought of as arising in the following way: An L wave front, emanating from the source, travels along the surface. To satisfy the boundary conditions, transverse waves are required to provide compensating surface tractions, and the energy to create these waves is steadily drawn from the L wave. The envelope of these transverse waves forms the head wave. These waves are well known in the study of plates and stratified media. While the theoretical basis of their existence in anisotropic media is well established,[16] the observations we report here appear to be the first unambiguous identification of head waves in single-crystal specimens. In Fig. 3 the predicted L and ST head-wave arrival is labeled HW. It merges smoothly into the ST wave at about 20° from epicenter. In the experimental scan image, beyond 20° the head wave can be clearly discerned, but not the ST wave which is too faint. The ST wave near epicenter and the head wave beyond 20° evolve smoothly into one another, giving the impression of being a single structure. In other experiments we find structures in equally good agreement with the predicted L and ST or L and

FT head-wave arrival. The interaction of head waves with surface features such as cracks deserves further study. A more detailed account of these results will be published elsewhere.

In conclusion, we have demonstrated that focusing has a profound influence on the amplitudes of ultrasonic waves propagated in elastically anisotropic solids when wide-angle point-source and point-detection is used. The scan images of silicon we have obtained contain a wealth of structures due to single and multipass modes and also well-defined features due to the passage of head waves. Although we are dealing with coherent wave forms, the most important features in our results are well accounted for in Monte Carlo simulations in which ray intensities are added without regard to phase. Our results are in accord with what is known about the wave surface and focusing pattern of silicon. Closer attention needs, however, to be given to surface-directivity effects and, more importantly, the dynamical Green's functions of anisotropic solids need to be evaluated for practical testing geometries.

The technique we have described is, in some regards, complementary to conventional phonon imaging. The natural advantages of phonon imaging lie in its access to fundamental processes at low temperatures and to the nonlinear region of the phonon-dispersion relation, its superior spatial resolution, and its applicability to relatively small samples. Scan imaging, on the other hand, is able to probe metals and composite materials in which ballistic phonon propagation is prevented by scattering effects. Moreover, it is a room-temperature technique and it provides good time resolution, which allows for the accurate determination of elastic constants and other material properties.

This work has been supported by the NSF-funded Materials Science Center at Cornell University. A.G.E. also acknowledges support from the University of the Witwatersrand; W.S. and K.Y.K. acknowledge the support of the ONR, Physical Acoustics Program.

[a]On leave from the University of the Witwatersrand, Johannesburg, South Africa.

[1]H. J. Maris, J. Acoust. Soc. Am. **50**, 812 (1971).

[2]H. J. Maris, in *Nonequilibrium Phonons in Nonmetallic Crystals,* edited by W. Eisenmenger and A. A. Kaplyanskii (North-Holland, Amsterdam, 1986), p. 51.

[3]G. A. Northrop and J. P. Wolfe, Phys. Rev. B **22**, 6196 (1980).

[4]G. A. Northrop and J. P. Wolfe, in *Nonequilibrium Phonon Dynamics,* edited by W. E. Bron (Plenum, New York, 1985), p. 165.

[5]G. F. D. Duff, Philos. Trans. Roy. Soc. London A **252**, 249 (1960).

[6]V. T. Buchwald, Proc. Roy. Soc. London A **253**, 563 (1959).

[7]W. Sachse and K. Y. Kim, in *Review of Quantitative Nondestructive Evaluation,* edited by D. O. Thompson and D. E. Chimenti (Plenum, New York, 1986), Vol. 6A, p. 311.

[8]D. A. Hutchins, in *Physical Acoustics,* edited by W. P. Mason and R. N. Thurston (Academic, Boston, 1988), Vol. 18, p. 21.

[9]A. N. Ceranoglu and Y. H. Pao, ASME J. Appl. Mech. **48**, 125 (1981); **48**, 133 (1981); **48**, 139 (1981).

[10]N. Cameron and G. Eason, Q. J. Mech. Appl. Math. **20**, 23 (1967).

[11]M. G. Cottam and A. A Maradudin, in *Surface Excitations,* edited by V. M. Agranovich and R. Loudon (Elsevier, Amsterdam, 1984), p. 1.

[12]B. A. Auld, *Acoustic Fields and Waves in Solids* (Wiley, New York, 1973), Vol. 1.

[13]The elastic constants and density of silicon for the calculations were taken from Ref. 12: $C_{11}=165.7$, $C_{12}=63.9$, $C_{44}=79.56$ GPa, and $\rho=2332$ kg/m^3.

[14]A. G. Every, Phys. Rev. B **33**, 2719 (1986).

[15]A. G. Every, Phys. Rev. B **24**, 3456 (1981); D. C. Hurley and J. P. Wolfe, Phys. Rev. B **32**, 2568 (1985).

[16]M. J. P. Musgrave and R. G. Payton, Q. J. Mech. Appl. Math. **34**, 235 (1981); **35**, 173 (1982).

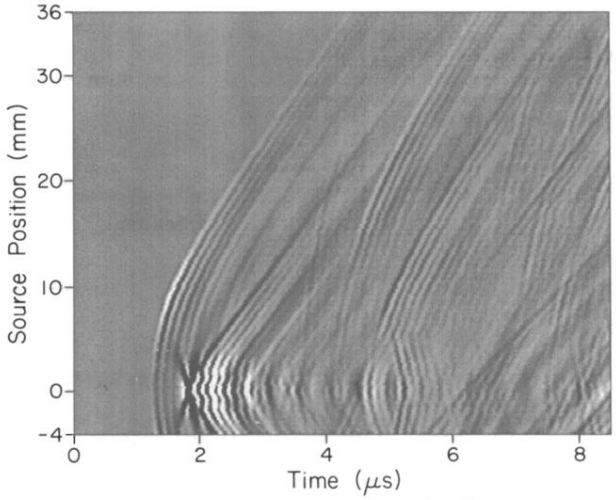

FIG. 2. A scan image obtained with a [100]-oriented silicon single crystal.

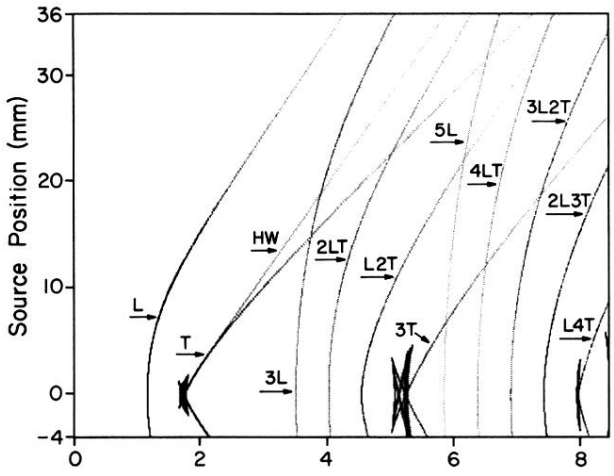

FIG. 3. Calculated scan image corresponding to Fig. 2.

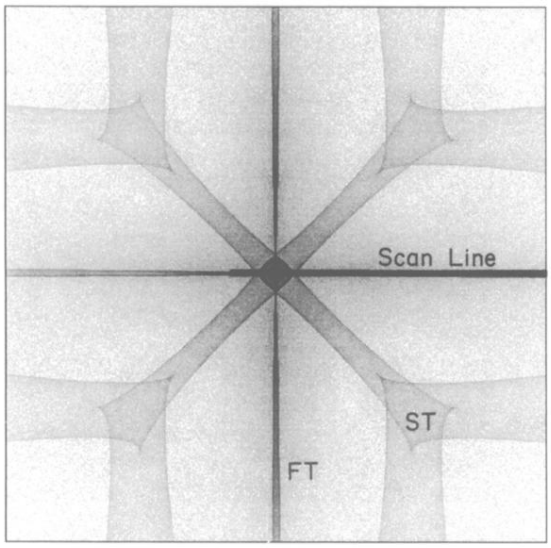

FIG. 4. Focusing pattern of ST and FT waves for a [100]-oriented silicon single crystal.